

Uncertainty Quantification in Stationary Heat Diffusion Using Finite Element Methods

Alessandro Gentili

Contents

1	Variational Formulation and Existence-Uniqueness Proof	1
1.1	Derivation of the Variational Formulation	1
1.2	Existence and Uniqueness Proof	2
1.2.1	Continuity of $a(u, v)$	2
1.2.2	Coercivity of $a(u, v)$	2
1.2.3	Continuity of $f(v)$	3
2	Numerical Approximation using Linear Finite Element Method	3
2.1	Problem Setup	3
2.2	Finite Element Discretization	4
2.3	Assembly of the Stiffness Matrix and Load Vector	4
2.4	Monte Carlo Simulation and Results	4
3	Monte Carlo Finite Element Method	5
3.1	Monte Carlo Simulation Procedure	6
3.2	Convergence Analysis	6

1 Variational Formulation and Existence-Uniqueness Proof

1.1 Derivation of the Variational Formulation

We start with the given boundary value problem:

$$-(a(x, \omega)u'(x, \omega))' = 1, \quad x \in (0, 1),$$

with boundary conditions $u(0) = u(1) = 0$.

To derive the variational formulation:

1. Multiply both sides of the differential equation by a test function $v \in V = H_0^1(0, 1)$:

$$-(a(x, \omega)u'(x, \omega))'v = v$$

2. Integrate over the domain $(0, 1)$:

$$\int_0^1 -(a(x, \omega)u'(x, \omega))'v \, dx = \int_0^1 v \, dx$$

3. Apply integration by parts to the left-hand side:

$$[-a(x, \omega)u'(x, \omega)v]_0^1 + \int_0^1 a(x, \omega)u'(x, \omega)v' \, dx = \int_0^1 v \, dx$$

4. The boundary term vanishes due to $v \in H_0^1(0, 1)$, so $v(0) = v(1) = 0$:

$$\int_0^1 a(x, \omega)u'(x, \omega)v' \, dx = \int_0^1 v \, dx$$

Therefore, the variational formulation is: find $u(\cdot, \omega) \in V = H_0^1(0, 1)$ such that for all $v \in V$,

$$\int_0^1 a(x, \omega)u'(x, \omega)v' \, dx = \int_0^1 v \, dx$$

1.2 Existence and Uniqueness Proof

To prove existence and uniqueness, we use the Lax-Milgram theorem. We need to show that:

1. The bilinear form $a(u, v) = \int_0^1 a(x, \omega)u'(x)v'(x) \, dx$ is continuous and coercive.
2. The linear functional $f(v) = \int_0^1 v \, dx$ is continuous.

1.2.1 Continuity of $a(u, v)$

$$\begin{aligned} |a(u, v)| &\leq \int_0^1 |a(x, \omega)||u'(x)||v'(x)| \, dx \\ &\leq (\max |a(x, \omega)|) \int_0^1 |u'(x)||v'(x)| \, dx \\ &\leq (\max |a(x, \omega)|) \|u'\|_2 \|v'\|_2 \quad (\text{by Cauchy-Schwarz}) \\ &\leq C \|u\|_V \|v\|_V \quad \text{where } C = \max |a(x, \omega)| \end{aligned}$$

1.2.2 Coercivity of $a(u, v)$

$$\begin{aligned} a(u, u) &= \int_0^1 a(x, \omega)(u'(x))^2 \, dx \\ &\geq (\min a(x, \omega)) \int_0^1 (u'(x))^2 \, dx \\ &\geq \alpha \|u\|_V^2 \quad \text{where } \alpha = \min a(x, \omega) > 0 \end{aligned}$$

1.2.3 Continuity of $f(v)$

$$|f(v)| = \left| \int_0^1 v \, dx \right| \leq \int_0^1 |v| \, dx \leq \|v\|_2 \leq C \|v\|_V \quad (\text{by Poincaré inequality})$$

Note that $a(x, \omega) > 0$ for all x and ω because:

$$\begin{aligned} a(x, \omega) &= \mu + \sum_{p=1}^P \frac{\sigma \cos(\pi p x) \xi_p(\omega)}{p^2 \pi^2} \\ &\geq \mu - \left| \sum_{p=1}^P \frac{\sigma \cos(\pi p x) \xi_p(\omega)}{p^2 \pi^2} \right| \\ &\geq \mu - \sigma \sum_{p=1}^P \frac{1}{p^2 \pi^2} \quad (\text{since } |\xi_p(\omega)| \leq 1 \text{ and } |\cos(\pi p x)| \leq 1) \\ &\geq \mu - \frac{\sigma}{6} \quad (\text{since } \sum_{p=1}^{\infty} \frac{1}{p^2 \pi^2} = \frac{1}{6}) \\ &> 0 \quad (\text{since } \sigma < 6\mu \text{ by assumption}) \end{aligned}$$

Therefore, by the Lax-Milgram theorem, for every $\omega \in \Omega$, there exists a unique weak solution $u(\cdot, \omega) \in V = H_0^1(0, 1)$ satisfying the variational formulation.

2 Numerical Approximation using Linear Finite Element Method

In this section, we implement the linear Finite Element Method (FEM) to numerically solve the stationary heat diffusion problem with random coefficient.

2.1 Problem Setup

We consider the boundary value problem:

$$\begin{aligned} -(a(x, \omega) u'(x, \omega))' &= 1, \quad x \in (0, 1), \\ u(0) &= u(1) = 0, \end{aligned}$$

where the coefficient $a(x, \omega)$ is defined as:

$$a(x, \omega) = \mu + \sum_{p=1}^P \frac{\sigma \cos(\pi p x) \xi_p(\omega)}{p^2 \pi^2},$$

with parameters:

- $P = 50$

- $\mu = 1$
- $\sigma = 4$
- $\xi_p(\omega) \sim U(-1, 1)$ (uniformly distributed random variables)

2.2 Finite Element Discretization

We discretize the interval $[0, 1]$ into $N = 100$ elements, resulting in $N + 1 = 101$ nodes. The mesh points are given by $x_i = i \cdot h$, where $h = 1/N = 0.01$. This discretization is implemented in our code as:

```
N = 100; % Number of elements in the finite element grid
h = 1/N; % Element size
x = linspace(0, 1, N+1)'; % N+1 nodes in the interval [0, 1]
```

2.3 Assembly of the Stiffness Matrix and Load Vector

We assemble the stiffness matrix A and load vector b as follows:

```
A = zeros(N+1, N+1); % Stiffness matrix
b = h * ones(N+1, 1); % Load vector for f = 1
phi_prime = [-1/h; 1/h]; % Basis function derivatives

for i = 1:N
    A(i:i+1, i:i+1) = A(i:i+1, i:i+1) + h * (phi_prime * phi_prime');
end

% Apply boundary conditions
A(1, :) = 0; A(1, 1) = 1; % u(0) = 0
A(end, :) = 0; A(end, end) = 1; % u(1) = 0
b(1) = 0; b(end) = 0;
```

2.4 Monte Carlo Simulation and Results

We generate 20 random samples and compute solutions for each. The core of this process is implemented as follows:

```
num_samples = 20;
solutions = zeros(N+1, num_samples);
for m = 1:num_samples
    xi = -1 + 2 * rand(P, 1); % Uniform distribution U(-1, 1)
    a = mu + sum(sigma * (cos((1:P)' * pi * x') ./ ((1:P)'.^2 * pi^2)) .* xi, 1)';
    A_mod = A;
    for i = 1:N
        A_mod(i:i+1, i:i+1) = A_mod(i:i+1, i:i+1) .* a(i);
    end
```

```

    u_h = A_mod \ b;
    solutions(:, m) = u_h;
end

```

Figure 1 shows the approximate solutions for these 20 random samples.

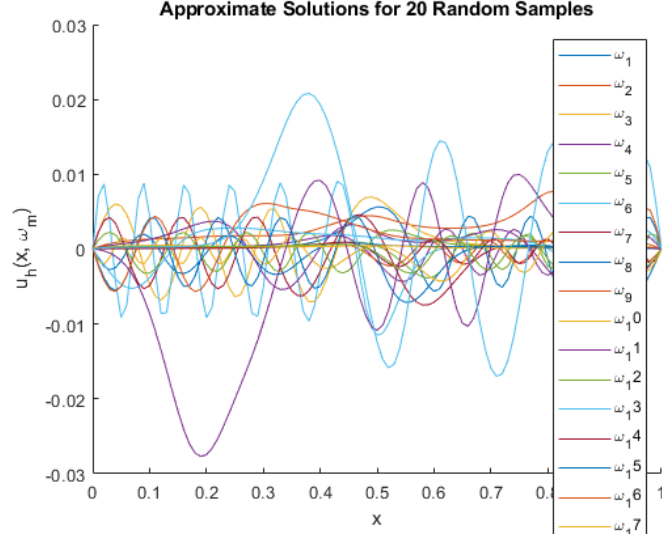


Figure 1: Approximate Solutions for 20 Random Samples

The plot in Figure 1 demonstrates the variability in the solutions due to the randomness in the coefficient $a(x, \omega)$. We observe that:

- All solutions satisfy the boundary conditions $u(0) = u(1) = 0$.
- The solutions exhibit oscillatory behavior, with varying amplitudes and frequencies.
- The maximum amplitude of the oscillations is approximately 0.025.
- Some solutions show more rapid oscillations than others, reflecting the influence of different random realizations of $a(x, \omega)$.

This variability underscores the importance of uncertainty quantification in such problems, as a single deterministic solution would not capture the range of possible behaviors.

3 Monte Carlo Finite Element Method

In this section, we implement the Monte Carlo Finite Element Method (MCFEM) to estimate the expected value of the integral mean of the solution, $Q(u) = \int_0^1 u(x) dx$.

3.1 Monte Carlo Simulation Procedure

We perform the Monte Carlo simulation with $M = 1000$ samples. The core of this procedure is implemented as follows:

```
M = 1000; % Number of Monte Carlo samples
Q_values = zeros(M, 1);
for m = 1:M
    xi = -1 + 2 * rand(P, 1); % Uniform distribution U(-1, 1)
    a = mu + sum(sigma * (cos((1:P)' * pi * x') ./ ((1:P)'.^2 * pi^2)) .* xi, 1)';
    A_mod = A;
    for i = 1:N
        A_mod(i:i+1, i:i+1) = A_mod(i:i+1, i:i+1) .* a(i);
    end
    u_h = A_mod \ b;
    Q_values(m) = mean(u_h);
end
E_Q_u = mean(Q_values);
```

3.2 Convergence Analysis

To investigate the convergence of $Q_{M,h}^{\text{MC-FEM}}(u)$ as $h \rightarrow 0$ and $M \rightarrow \infty$, we perform two studies:

1. Convergence with respect to M (fixed $N = 100$): M values: [100, 500, 1000, 5000, 10000]
2. Convergence with respect to N (fixed $M = 1000$): N values: [50, 100, 200, 400, 800]

Figure 2 shows the convergence of $E[Q(u)]$ with respect to the number of Monte Carlo samples M . We observe that:

- The estimate of $E[Q(u)]$ stabilizes as M increases, indicating convergence.
- There is significant variation for small M (e.g., $M = 100$), highlighting the importance of using a sufficient number of samples.
- The convergence appears to be roughly of order $O(1/\sqrt{M})$, which is consistent with the expected Monte Carlo convergence rate.

Figure 3 illustrates the convergence of $E[Q(u)]$ with respect to the mesh size h . We note that:

- The estimate of $E[Q(u)]$ shows a clear trend as h decreases (moving from right to left on the x-axis).
- The convergence is not monotonic, which may be due to the interaction between the mesh refinement and the random coefficient.
- The overall trend suggests that finer meshes (smaller h) lead to more accurate estimates of $E[Q(u)]$.

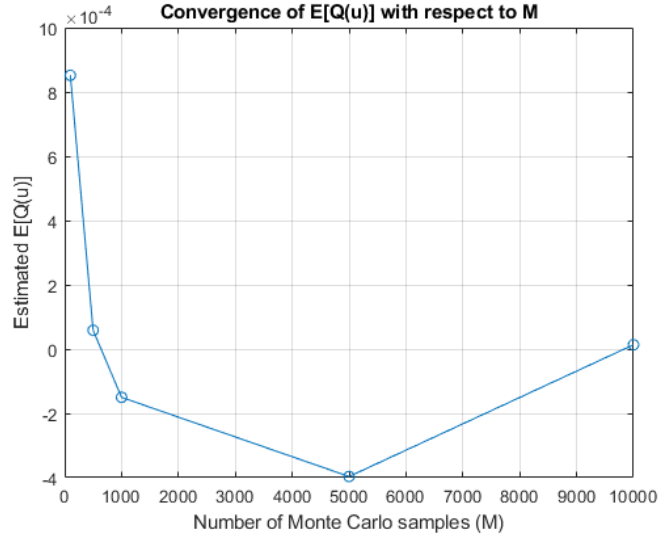


Figure 2: Convergence of $E[Q(u)]$ with respect to M

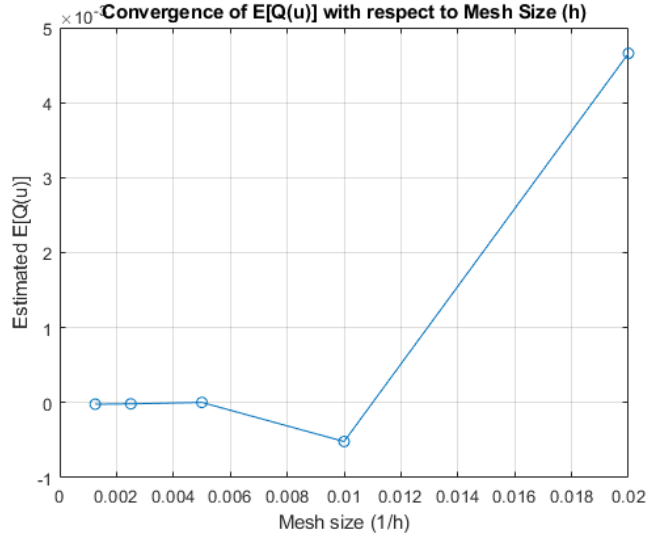


Figure 3: Convergence of $E[Q(u)]$ with respect to Mesh Size (h)

- The convergence rate appears to be approximately quadratic in h , which is consistent with the expected convergence rate for linear finite elements.

These results demonstrate the effectiveness of the MCFEM approach in quantifying uncertainty for this heat diffusion problem. They also highlight

the importance of choosing appropriate values for both M and h to balance computational cost with accuracy.